Influence of stratospheric aerosol geoengineering on temperature mean and precipitation extremes indices in Africa

Salomon Obahoundje, Vami Hermann N'guessan Bi, Arona Diedhiou, Ben Kravitz and John C. Moore
(Author affiliations can be found at the end of the article)

Received 19 March 2021
Revised 7 October 2021
9 March 2022
3 April 2022
Accepted 3 May 2022

Abstract

Purpose – Three Coupled Model Intercomparison Project Phase 5 models involved in the G4 experiment of the Geoengineering Model Inter-comparison Project (GeoMIP) project were used to investigate the impact of stratospheric aerosol injection (SAI) on the mean surface air temperature and precipitation extremes in Africa.

Design/methodology/approach – This impact was examined under G4 and Representative Concentration Pathway (RCP) 4.5 scenarios on the total precipitation, the number of rainy days (RR1) and of days with heavy rainfall (R20 mm), the rainfall intensity (SDII), the maximum length of consecutive wet (CWD) and dry (CDD) days and on the maximum rainfall in five consecutive days (Rx5day) across four regions: Western Africa (WAF), Eastern Africa (EAF), Northern Africa and Southern Africa (SAF).

Findings – During the 50 years (2020–2069) of SAI, mean continental warming is −0.40°C lower in G4 than under RCP4.5. During the post-injection period (2070–2090), the temperature continues to increase, but at a lower rate (−0.19°C) than in RCP4.5. During SAI, annual rainfall in G4 is significantly greater than in RCP4.5 over the high latitudes (especially over SAF) and lower over the tropics. The termination of SAI leads to a significant increase of rainfall over Sahel and EAF and a decrease over SAF and Guinea Coast (WAF).

Practical implications – Compared to RCP4.5, SAI will contribute to reducing significantly regional warming but with a significant decrease of rainfall in the tropics where rainfed agriculture account for a large part of the economies. After the SAI period, the risk of drought over the extratropical regions (especially in SAF) will be mitigated, while the risk of floods will be exacerbated in the Central Sahel.

Originality/value – To meet the Paris Agreement, African countries will implement mitigation measures to contribute to keep the surface air temperature below 2°C. Geoengineering with SAI is suggested as an

The research undertaken by the Côte d'Ivoire team in Africa and leading to this publication has received the financial support of the DECIMALS fund of the Solar Radiation Management Governance Initiative, set up by the Royal Society, Environmental Defense Fund and The World Academy of Sciences (TWAS) and funded by the Open Philanthropy Project. This research on the impact of SRM in Africa is co-funded by Institut de Recherche pour le Développement (Institut de recherche pour le développement (IRD); France) grant number UMR IGE Imputation 252RA5. The GeoMIP data used in this study are open data available via the Earth System Grid. Support for B.K. was provided in part by the National Science Foundation through agreement CBET-1931641, the Indiana University Environmental Resilience Institute and the *Prepared for Environmental Change* Grand Challenge initiative.

International Journal of Climate Change Strategies and Management
Vol. 14 No. 4, 2022
pp. 399-423
Emerald Publishing Limited
1756-8692
DOI 10.1108/IJCCSM-03-2021-0028

option to meet this challenge, but its implication on the African climate system needs a deep investigation in the aim to understand the impacts on temperature and precipitation extremes. To the best of the authors' knowledge, this study is the first to investigate the potential impact of SAI using the G4 experiment of GeoMIP on temperature and precipitation extremes of the African continent.

Keywords Stratospheric aerosol injection, GeoMIP, Africa, Temperature, Precipitation, Climate extremes

Paper type Research paper

1. Introduction

Climate extremes especially related to temperature and precipitation variables are becoming common these past decades over the globe. The cold nights and days have decreased associated with increasing warm nights and days over the globe. The increasing heavy precipitation days are noted due to the increase in the number of very wet days, daily precipitation intensity as well as reduction of the number of consecutive dry days (Sillmann and Roeckner, 2008; Zhang *et al.*, 2011). These extremes are attributed to the changes in weather and climate events inputted by either human-induced climate change (Sillmann and Roeckner, 2008) or natural variability or else (Trenberth *et al.*, 2015). However, the occurrence, as well as the intensity and magnitude of these extremes, may vary from a region to another.

The African continent is already experiencing the adverse impacts of climate extremes events (Paeth *et al.*, 2011; Donat *et al.*, 2020), namely, precipitation extremes responsible for floods and droughts and temperature extremes causing heatwaves. They are disastrous for African populations and infrastructures (Di Baldassarre *et al.*, 2010) causing health issues (Du *et al.*, 2010) and economic loss.

Droughts have become frequent in the Guinea Coast of Western Africa (WAF) (Sylla *et al.*, 2016), in the Greater Horn of Eastern African (EAF) region (Somalia, Ethiopia, Kenya, Sudan and Tanzania) (Gebremeskel *et al.*, 2019; Gebremeskel Haile *et al.*, 2020) and Southern Africa (SAF) (Orimoloye *et al.*, 2019). These dry spells have caused water and electricity supply disruption (Gannon *et al.*, 2018) affecting all the activities sectors depending on water and energy and have led to crops failure as the agriculture practice is largely rainfed and thus increases food security challenges (Kogan *et al.*, 2019).

Likewise, flooding event has become common in the continent especially in Central Sahel of WAF region and is also associated with health issues (Kogan *et al.*, 2019) leading to human fatalities. Aside from droughts and floods extremes associated with civil conflicts in the continent (Von Uexkull, 2014), the temperature extremes have also impacted the African population these past decades. A significant rise in temperature extremes has been observed between 1979 and 2010 (Collins, 2011) impacting the health sector and energy sector from demand to distribution through production (Mideksa and Kallbekken, 2010; Ndiaye *et al.*, 2017).

A significant increase worldwide is projected for all the temperature-related extremes indices, namely, minimum and maximum, and the frequency of tropical nights as well as for specific extreme precipitation-based indices, namely, the maximum five-day precipitation and the 95th percentile of precipitation (Sillmann and Roeckner, 2008) which could affect all livelihood of the community. Specifically, Climate change due to global warming will likely affect all human life sectors in Africa, from water resources, agriculture (Roudier *et al.*, 2011) and food security (Thomas-Hope, 2018), to energy, peace and security (Brown and Crawford, 2008a, 2008b; Burke *et al.*, 2009). To mitigate these climate impacts, some measures have been set into place by African governments. All African nations have signed the 2015 Paris Climate Agreement intending to hold global temperature increases to "well below 2°C" and to pursue efforts to limit warming to “1.5°C above preindustrial levels”(Chin-Yee, 2016) and have accepted the nationally Determined Contributions to emissions reductions. Nevertheless, at regional scales, temperature increases in the African continent are projected to be higher than the global mean temperature increase under the Representative Concentration Pathway (RCP) 8.5 scenario (Nikulin *et al.*, 2018; Weber *et al.*, 2018). Weber *et al.* (2018) and Nikulin *et al.* (2018) demonstrated that even if the global temperature is kept below 2°C, African regions are projected to experience an increase in extreme temperature, longer and more frequent heatwaves as well as an increase in daily precipitation intensity of wet days. Longer dry spells are projected at 1.5°C in the Western Sahel subregion of West Africa (Diedhiou *et al.*, 2018) and 2°C of global warming. Diedhiou *et al.* (2018) also show that over the Central Sahel subregion of West Africa, despite a large ensemble spread, most models project an increase of total precipitation and heavy rainfall with risks of floods above 2°C. Therefore, Sub-Saharan African regions could meet serious food security issues (Parkes *et al.*, 2018) above 2°C.

The primary means of limiting temperature rise is reducing greenhouse gas emissions. However, if this does not do enough to address climate change, two additional measures have been proposed as ideas to further prevent risks from climate change, namely, carbon dioxide removal (CDR) and solar radiation management (SRM) (Rahm, 2018). Commercial CDR solutions already exist but not at large enough scale to deal with the enormity of the problem of climate change, and serious questions remain regarding its cost. Stratospheric Aerosol Albedo Modification by injection of sulphur in the stratosphere also called stratospheric aerosol injection (SAI) is a type of SRM, has recently received increased attention as a way to reduce global temperatures. Indeed, SAI is a proposed method for reducing human-induced climate change by spraying large quantities of tiny reflective particles into the stratosphere, an upper layer of the Earth’s atmosphere, to cool the planet by reflecting sunlight into space. This idea, which falls under the broader umbrella of geoengineering, aims to imitate volcanic eruptions which are known to cool the atmosphere (Budyko, 1977; Crutzen, 2006). A recent example is the eruption of Mt. Pinatubo in 1991, which injected approximately 20 megatons of sulphur dioxide into the atmosphere, leading to the cooling of the planet and with it, associated climate impacts (Robock, 2000; Rahm, 2018).

Atmospheric models have shown a wide range of climate sensitivity and differences in the response to stratospheric volcanic aerosols, with large uncertainties regarding its estimated climate effects (Visioni *et al.*, 2017). This wide range is partly because the forcing efficiency is sensitive to the injected amount of SO_2, the injection height and the spatiotemporal pattern of the injection (Kleinschmitt *et al.*, 2018). However, regardless of how SAI might be deployed, it will likely produce unequal regional impacts (Ferraro *et al.*, 2014). Although SAI is effective at reducing global mean precipitation increases from greenhouse gases (Ferraro *et al.*, 2014; Ferraro and Griffiths, 2016), the effectiveness of SAI in compensating for greenhouse gas-induced temperature change is considerably higher than for precipitation (Yu *et al.*, 2015). Thus, far there have been few studies investigating how SAI may affect characteristics and variability of precipitation and temperature over African regions (Pinto *et al.*, 2020). Especially, there is a lack of scientific information on what are the implications of SAI on mean temperature and how the SAI will affect the total precipitation and extremes during and after injection over African regions. Finally, how these effects may affect the livelihood of the communities remain a crucial question for efficiency of adaptation and mitigation policies and for sustainable development.

This study aims to explore the effects of SAI on the African continent under experiment G4 (described below) of the Geoengineering Model Inter-comparison Project (GeoMIP; Kravitz *et al.*, 2011). The phase 1 GeoMIP SAI experiments are G3 and G4 and specify injection of SO_2 from

2020 to 2069. In contrast, the G1 experiment is designed to explore more extreme SRM responses, by reducing incoming solar insolation, to greenhouse gas forcing of an instantaneous quadrupling of CO_2 concentration relative to pre-industrial levels, while under the G2 experiment, the positive radiative forcing of a 1% annual increase in CO_2 concentration is balanced by a decrease in the solar constant to year 50. The G3 experiment is designed to approximately balance the positive radiative forcing of the RCP4.5 scenario by a gradual injection of SO_2 or sulphate aerosols into the tropical lower stratosphere, while the G4 experiment, is also based on the RCP4.5 scenario, where an immediate negative radiative forcing is produced by an injection of SO_2 into the tropical lower stratosphere at a rate of 5 Tg per year. It is worth noting that the RCP 4.5 is a scenario that stabilises radiative forcing at 4.5 W m^{-2} in the year 2100 without ever exceeding that value, and that this scenario is rather close to the emissions specified under the 2015 Paris National Determined Contributions (NDCs) (Kitous and Keramidas, 2015). The G4 experiment is used for this study as it has been simulated by wide range of climate models, and its impacts discussed in many publications, for example, in the special collection (https://acp.copernicus.org/articles/special_issue376.html). In particular, it aims to answer the specific questions hereafter: What are the implications of SAI under the G4 experiment on mean temperature and precipitation in Africa and each subregion? What are the impacts of SAI on precipitation extreme indices? What is the effect of the termination of SAI on the mean and extreme climate indices? Finally, what are the implications of geoengineering in the G4 experiment compared to RCP4.5? The present study aims to investigate the influence of stratospheric aerosol geoengineering on temperature mean and precipitation extremes indices in Africa. This paper is structured as follows: Section 2 presents the data and the methods used in this study. Section 3 shows the results, starting with the implications of SAI on the warming of surface temperature and then, on the impact on the precipitation mean and extreme indices in Africa and its different subregions. Section 4 presents the discussion and the conclusion.

2. Data and methods

The temperature and precipitation results from three models that simulated GeoMIP experiment G4 (Kravitz *et al.*, 2011) were evaluated. This experiment involves daily injections of a constant amount of SO_2 at a rate of 5 Tg yr^{-1} of SO_2 into the lower stratosphere (approximately 16–25 km in altitude) at one point on the Equator from the year 2020 to 2069 against a background scenario of RCP4.5 (Figure 1). The injected sulphur dioxide gas (SO_2) reacts with water in the atmosphere (stratosphere) and the hydroxide (OH) from its oxidation produces the supercooled H_2O-H_2SO_4 particles which in turn form a persistent haze of liquid droplets, reflecting away sunlight and cooling the earth for a year or two. Then, the continuous injection may help to keep the Earth cool for a probably long period. This justifies the choice of 50 years (2020–2069) for the SAI experimentations. SAI stops in 2069, but the experiment continues for a further 20 years to 2089 with only GHG forcing as specified by RCP4.5 (Kravitz *et al.*, 2011).

Precipitation and temperature changes were first assessed at annual time scales. The future change is computed as the difference between the mean over the future (two separate periods: near and far) and the historical period. The near future is defined as the average over 2030–2050, and the far future is defined as the average over 2070–2090. The near future is aimed at capturing the dominant effects of SAI as compared to RCP4.5, and the far future is aimed at capturing the effects after SAI is abruptly terminated.

Then, the difference between G4 and RCP4.5 is computed for near and far future periods. A Student's *t*-test is used to evaluate the significance of the mean differences between the two simulations (G4 and RCP4.5) and periods. The advantages of a Student's *t*-test for such applications are described by Lydersen (2015). Details for its computation are given by

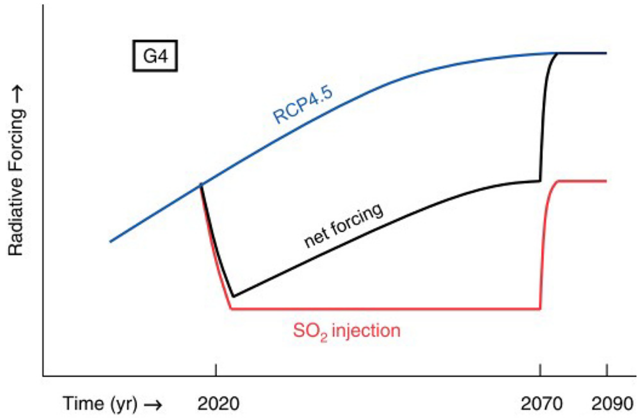

Note: This experiment is based on the RCP4.5 scenario, where immediate negative radiative forcing is produced by an injection of SO_2 into the tropical lower stratosphere at a rate of 5 Tg per year

Figure 1. Schematic of experiment G4, reproduced from Kravitz *et al.* (2011)

Janssen (2005). For analyses presented here over two periods of 21 years (2030–2050 for changes during the SAI period and 2070–2090 for changes after the injection period) statistically, significant values are computed at the 95% confidence level. The degrees of freedom are 40 for changes between simulations and 20 when computing future changes relative to the historical period (1976–2005).

The models used in this study are presented in Table 1. The basic description of each model can be seen under the reference column of Table 1 as well as on the IPCC fifth assessment report (Kattsov *et al.*, 2013).

The different African subregions evaluated in this study are presented in Figure 2, and their geographical boundaries are summarised in Table 2. These subregions are those identified in the IPCC Special Report on Managing the Risks of Extreme Events and Disasters to Advance Climate Change Adaptation (SREX) regions (Giorgi and Francisco, 2000; Seneviratne *et al.*, 2012).

To capture the distribution of precipitation spells, six climate extremes indices proposed and presented in the World Meteorological Organisation (WMO) guideline (Klein Tank *et al.*, 2009) were computed. Those indices are the maximum length of consecutive wet days (CWD), highest precipitation amount in five consecutive days (RX5day) the maximum length of consecutive dry days (CDD), the number of days per year with rainfall (RR) ≥1 mm (RR1), the simple daily intensity index (SDII) and the number of days per year with RR ≥20 mm (R20mm). The definitions of those indices are presented in Table 3. The selected indices were computed as recommended by the WMO guideline (World Meteorological

Table 1. Climate models used in this study

Models	Reference	Horizontal resolution
CanESM2	Arora *et al.* (2011)	2.81°
MIROC-ESM	Watanabe *et al.* (2011)	2.81°
MIROC-ESM-CHEM	Watanabe *et al.* (2011)	2.81°

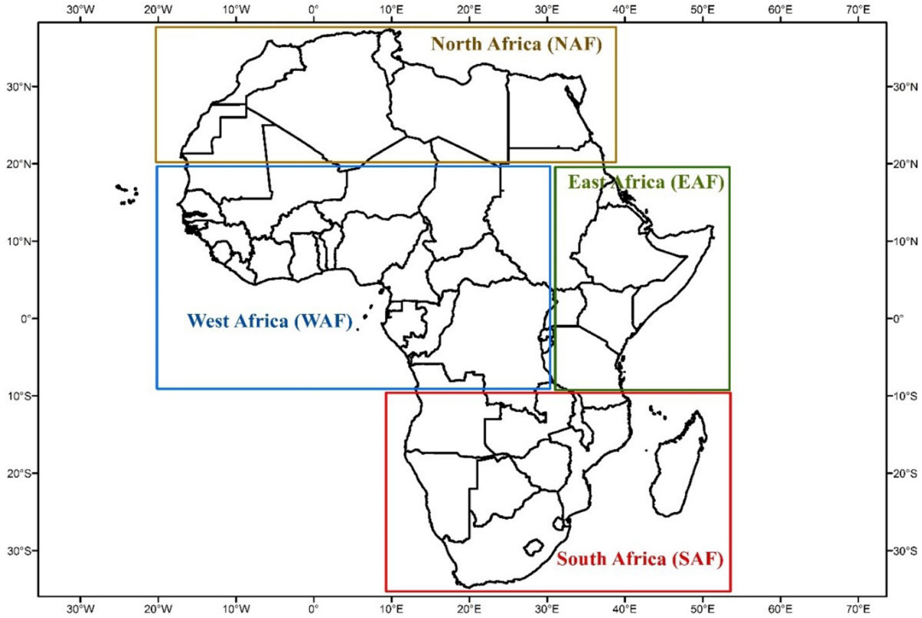

Figure 2.
Map of African countries with subregions

Table 2.
Definitions of African subregions for this study

Regions	Longitude	Latitude
East Africa (EAF)	30 – 52E	10S – 20 N
North Africa (NAF)	18W – 40E	20 – 38 N
South Africa (SAF)	10 – 52E	10 – 36 S
West Africa (WAF)	18W – 30E	10S – 20 N

Table 3.
Precipitation extreme indices

Index	Unit	Description	Definition
CWD	days	Consecutive wet days	The maximum length of wet spell (RR ≥1 mm)
RX5day	mm	Highest precipitation amount in 5 consecutive days	Annual maximum precipitation sums on five-day intervals
CDD	days	Consecutive dry days	Maximum length of dry spell (RR <1 mm)
RR1	Days	Wet days	Number of days per year with rainfall (RR) ≥1 mm
SDII	mm/day	Simple daily intensity index	Annual total precipitation divided by number of wet days (≥1 mm). If W represents the number of wet days in j then the simple precipitation intensity index SDIIj = sum (RRwj)/W
R20mm	days	Very heavy precipitation days	The number of days per year with RR ≥20 mm

Organization, 2018) established by the Task Team on the Definition of Extreme Weather and Climate Events. These indices were widely used for the investigation of climate extremes at a regional scale (Lima *et al.*, 2014; Peterson *et al.*, 2001) and global scale (Hartmann *et al.*, 2013; Herring *et al.*, 2014; Seneviratne *et al.*, 2012; Sönke *et al.*, 2015).

3. Results

3.1 Implication of stratospheric aerosol injection on surface air temperature

Figure 3 shows the average air temperature change as compared to a historical period (Hist; 1976–2005 average) of each model for the near (2030–2050) and far (2070–2090) futures. Over both future periods under the G4 experiment, the temperature is projected to increase significantly but at a lower rate during the near future [during the injection period, Figure 3(a)–(d)] than during the far future after the injection has stopped [Figure 3(e)–(h)]. It is important to highlight that the changes are not significant over coastal countries from Senegal to Benin and south-western of Nigeria for both futures periods considering the model ensemble mean [Figure 3(d) and (h)].

Figure 4 (a)–(h) displays the difference between experiments (G4 minus RCP4.5) for all the models (plus the ensemble mean) over the near (a–d) and far (e–h) futures. The analysis reveals that all models project a cooling effect of the G4 experiment over the entire continent,

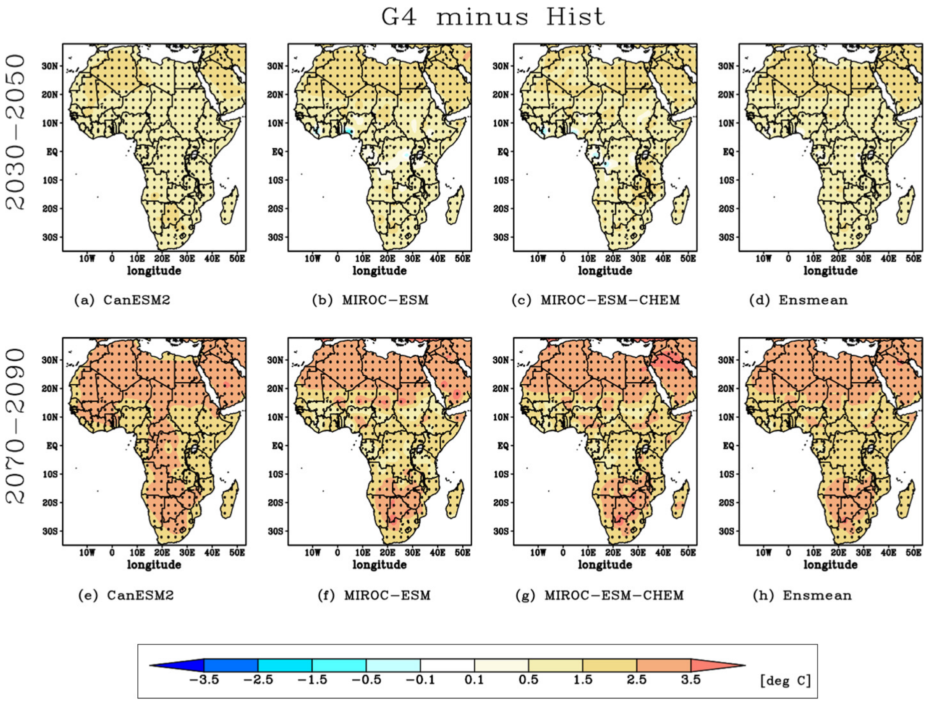

Notes: [Top row, Figure 3(a)–(d), in the SAI period] and for the far future 2070–2090 [bottom row, Figure 3 (e)–(h), in the Post-SAI period]. the historical period is taken to be the average over 1976–2005. The black dots refer to the areas where the changes are statistically significant at 95% confidence level

Figure 3. Changes (G4 minus historical) of surface air temperature for each model (from left to right column: CanESM2, MIROC-ESM, MIROC-ESM-CHEM and the ensemble mean, respectively) for the near future 2030–2050

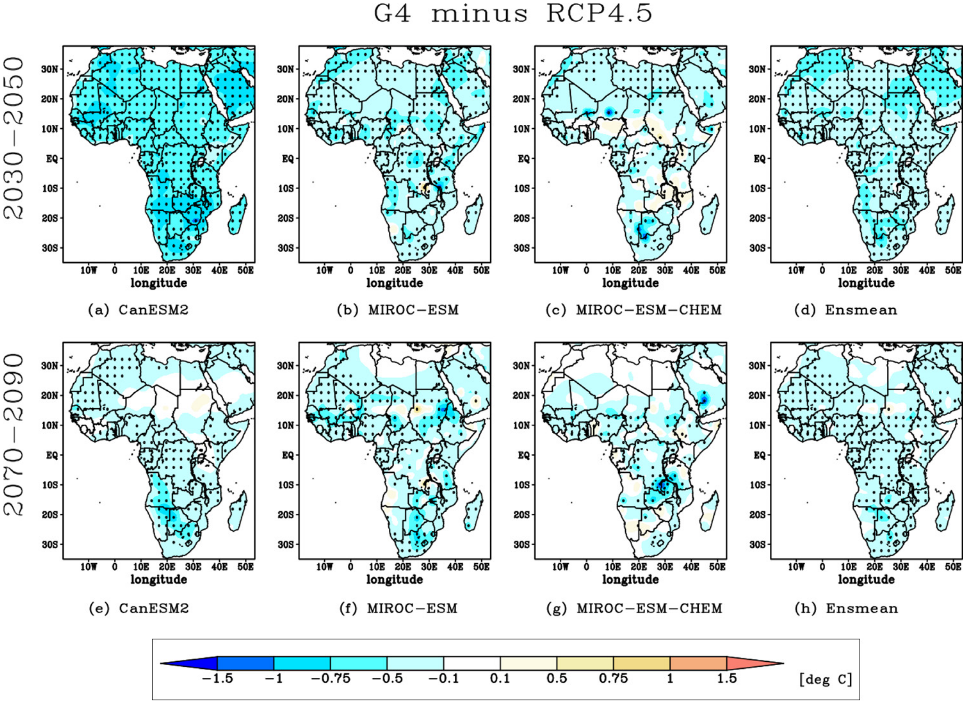

Figure 4.
Changes in surface air temperature between G4 and RCP4.5 (G4 minus RCP4.5) for each model (from left to right column: CanESM2, MIROC-ESM, MIROC-ESM-CHEM and Ensemble mean, respectively) for the near future 2030–2050

Notes: [top row, Figure 3(a)–(d), in the SAI period] and for the far future 2070–2090 [bottom row, Figure 3 (e)–(h), in the Post-SAI period]. the black dots in the maps stand for areas with significant changes at 95% confidence level

but the cooling is stronger during the near future (the period of injection) than in the far future (after the injection has ceased). The magnitude of the cooling varies according to the models and the subregions. During the near future period (injection period), all the models, as well as their ensemble mean present significant cooling (compared to RCP4.5) over the entire continent except with the an atmospheric chemistry coupled version of MIROC-ESM model which shows weak warming over the tropics in some parts of sub-Saharan regions [north-eastern of Nigeria, South of Tchad, South Sudan and south-eastern part of the continent, see Figure 4(c)]. The ensemble mean [Figure 4(d)] shows that cooling due to SAI in the near future varies up to 0.75°C depending on the subregions with a mean cooling of 0.37°C for the whole continent.

During the far future (after the injection period), the area of a statistically significant cooling is reduced to a major part of the sub-Saharan region and the western side of the Northern African (NAF) subregion. The ensemble mean [Figure 4(h)] shows that the warming in the G4 simulation will be weaker than in RCP4.5 and the difference between both simulations could vary up to 0.5°C depending on the subregion (over WAF and EAF and in the central part of SAF) with a mean cooling of 0.19°C for the whole continent.

The average temperature differences (G4-RCP4.5) for each of these periods per region are presented in Figure 5. Over Eastern Africa (EAF), the air temperature change ranges from

0.13°C to −0.59°C during the injection period (near future) and from −0.17°C to −0.23°C during the far future. Over NAF, the cooling ranges from −0.41°C to −0.63°C during the injection period and from 0 to −0.17°C after the SAI period. Over SAF, the cooling ranges from −0.14°C to −0.63°C during the SAI period and from −0.15°C to −0.34°C during the far future. Over WAF region, the air temperature cooling ranges from −0.08°C to −0.58°C during the injection period and from −0.17°C to −0.35°C during the far future. Overall, compared to RCP4.5, the SAI reduces air temperature warming in all African regions and the magnitude of this cooling is generally greater during the injection phase than after the termination of the SAI experiment.

In summary, during the 50 years (2020–2069) of injection period, mean continental warming is −0.40°C lower in G4 than under RCP4.5. During the 20 years post-injection period (2070–2090), surface air temperature continues to increase at a higher rate (+1,2°C) than during the SAI period in G4 (2030–2050), but at a lower rate (−0.19°C) than in RCP4.5 (2070–2090).

3.2 Impact of stratospheric aerosol injection on mean precipitation

Figure 6 displays from left to right, annual precipitation change between G4 and RCP4.5 during the injection period [Figure 6(a)], between far future (after the injection period) and the injection period in G4 simulations [Figure 6(b)], between G4 and RCP4.5 in the far future [Figure 6(c), after the injection period] and between far future and the injection period in RCP4.5 simulations [Figure 6(d)].

During the injection period (2030–2050), when comparing G4 and RCP4.5 [Figure 6(a)], a significant increase is noted in the total annual precipitation over the high latitudes (NAF and SAF) while a decrease is simulated in the tropical band especially over EAF region. Indeed, as the SAI experiment consists of cooling air temperature through aerosol injection in the stratosphere, it is suggested that this could affect convective activity in the Intertropical Convergence Zone (ITCZ) and the intensity of Hadley Circulation, leading to a

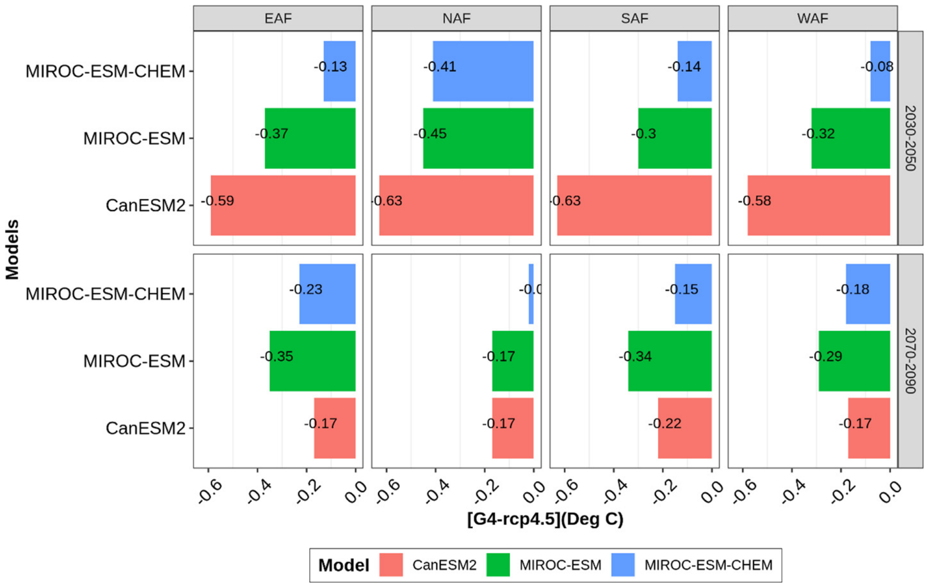

Figure 5.
Changes in surface air temperature between G4 and RCP4.5 (G4 minus RCP4.5) for each model-averaged per region for near future (top row, in the SAI period) and far future (bottom row, in the Post-SAI period). From left to right: EAF, NAF, SAF, WAF

decline in total precipitation in the tropical band (WAF and especially in EAF) and an increase in total precipitation over extratropical regions (NAF and SAF), greater over SAF than NAF.

After the termination of SAI [Figure 6(b), in G4 simulations], the precipitation will increase significantly over the Sahelian band of WAF, over EAF and Southern part of NAF, while a significant decrease is noted over SAF and Guinea Coast of WAF. No significant changes are found in the northern part of NAF. However, [Figure 6(c)] shows that after the injection period, the annual precipitation will remain greater in G4 than in RCP4.5 simulations almost everywhere, except over Guinea Coast of WAF and in EAF (over Great Lakes region and the Horn of Africa).

When comparing the 2070–2090 period to the 2030–2050 period in each experiment [Figure 6(b) for G4 and Figure 6(d) for RCP4.5], precipitation will significantly increase in WAF, EAF and in large part of NAF, while SAF will experience a significant shift of annual rainfall relatively more intense in G4 than in RCP4.5. However, analyses of changes inside each set of simulations relative to the historical period (Appendix Figure A1) show that the increase of precipitation will be greater in G4 than in RCP4.5 over WAF, EAF and NAF, but the decrease of rainfall over SAF will be lower in G4 than in RCP4.5.

Nevertheless, it is important to highlight that the projected precipitation deficit in the far future over SAF in RCP4.5 [Figure 6(d)] and in RCP8.5 over NAF (Waha *et al.*, 2017) and in the western area of WAF (Diedhiou *et al.*, 2018) will be mitigated during the SAI and in large part after the termination [G4 simulations, Figure 6(c)] as well as the risk of floods and landslides projected in RCP4.5 [Figure 6(d)] and RCP8.5 (Diedhiou *et al.*, 2018) over Guinea Highlands (in WAF) and in EAF (Great Lake regions and Horn of Africa; Osima *et al.*, 2018). The termination of SAI may increase the risk of floods projected over Central Sahel of WAF in RCP4.5 [Figure 6 (d)] and RCP8.5 (Diedhiou *et al.*, 2018) due to a significant increase of total annual precipitation [Figure 6(b), 6(c)]. NAF projected to be prone to drought in RCP8.5 (Waha *et al.*, 2017) will be wetter in RCP4.5 [Figure 6(d)] and will experience at its central and southern part more rainy events during the injection and mainly after the SAI period [Figure 6(a), 6(c) and 6(d)].

3.3 Impacts of stratospheric aerosol injection on precipitation intensity and number of rainy days

Figure 7 presents the changes in the number of days per year with rainfall RR $\geq$1 mm [RR1; Figure 7(a)–7(d)], SDII[Figure 7(e)–7(h)] and in the number of days per year with RR $\geq$ 20 mm [R20mm; Figure 7(i)–7(l)].

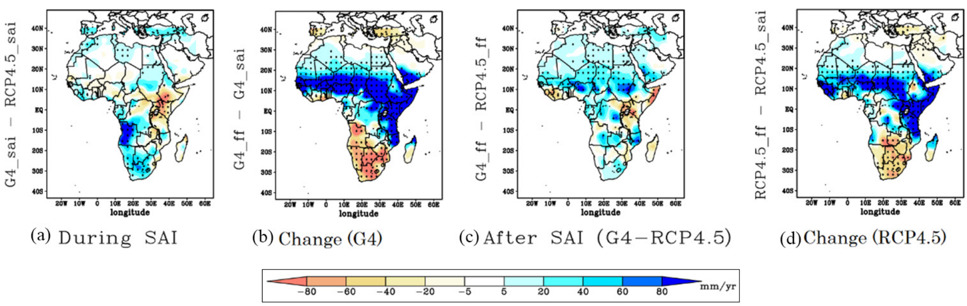

Figure 6.
Change in precipitation in the ensemble mean of three models (from left to right column: G4_sai minus RCP4.5_sai, G4_ff minus G4_sai, G4_ff minus RCP4.5_ff and RCP4.5_ff minus G4_sai) for the near future 2030–2050 (SAI) and for the far future 2070–2090 (ff)

Note: Black dots on the maps delimit areas with significant changes at 95% confidence level

During the injection period, the number of wet days is significantly greater in G4 than in RCP4.5 over the WAF region, along the western side of SAF and along the northern side of NAF [Figure 7(a)] compared to RCP4.5 in the same period. In contrast, the EAF region has a weaker number of wet days under G4 compared to RCP4.5 except in northern parts of Sudan and Ethiopia [Figure 7(a)]. The termination of SAI will lead in 2070–2090 (compared to 2030–2050 period in G4) to a significant increase of rainy days in WAF with maxima in Central Sahel and over EAF and to a significant decrease of wet days over the Guinea Gulf of WAF, Central Africa, SAF and northern part of NAF [Figure 7(b)]. However, the number of rainy days due to the termination effect in G4 will be greater than that of the projected number of wet days in RCP4.5 in the whole Africa (with significant maxima over Central Sahel and the Sahara Desert) except over EAF and the Guinea Highlands in WAF [Figure 7(c)], meaning that over SAF and northern NAF, the projected deficit of wet days in RCP4.5 during 2070–2090 period will be mitigated with the termination effect [Figure 7(c), (d)].

During the injection period, the intensity of rainfall (SDII) does not show any significant changes in the whole of Africa [Figure 7(e)] compared to RCP4.5 in the same period. However, a slight decrease can be noted in the tropical band (WAF and EAF) and a weak increase of SDII in the high latitudes (NAF and SAF). The termination of SAI will lead in 2070–2090 (compared to the 2030–2050 period in G4) to a significant increase of SDII in WAF with maxima in Central Sahel and over EAF and NAF and a slight decrease of the intensity over SAF [Figure 7(f)]. The intensity of rainfall due to the termination effect in G4 will not change significantly compared to that of the projected SDII in RCP4.5, except over NAF where a significant increase is noted [Figure 7(g)]. This suggests over NAF, the mitigation of rainfall deficit projected in RCP4.5 during the 2070–2090 period due to the termination effect is associated with an increase of rainfall intensity [Figure 7(g), 7(h)].

During the injection period, the number of days with heavy rainfall (R20mm) does not show any significant changes in the whole of Africa [Figure 7(i)] compared to RCP4.5 in the same period. However, a slight decrease can be noted in the tropical band (WAF and EAF) and an increase of R20mm is simulated over SAF. The termination of SAI will lead in 2070–2090 (compared to the 2030–2050 period in G4) to a significant increase of days with heavy rainfall in WAF with maxima in Central Sahel and over EAF and a significant decrease of R20mm over SAF [Figure 7(j)]. The number of days with heavy rainfall due to the termination effect in G4 will be greater over WAF, EAF and SAF compared to that of the projected R20mm in RCP4.5, except over Guinea Coast of WAF and in the Greater Horn of EAF, where a significant a decrease is noted [Figure 7(g)]. This suggests that over SAF, the mitigation of rainfall deficit projected in RCP4.5 during the 2070–2090 period due to the termination effect is associated with an increase in the number of days with heavy rainfall [Figure 7(g), 7(h)].

In summary, compared to RCP4.5, Figure 7 shows that the SAI will lead to a decrease in rainfall in the tropics and an increase in rainfall in the African high latitudes. The termination effect will increase the risk of floods in the Central Sahel in G4 due to an increase in the number of wet days and of very heavy precipitation days, while the risk of drought will be mitigated over the extratropical regions (especially in SAF) due to an increase of the number of rainy days (Western part of SAF), the rainfall intensity (over NAF) and the number of days with very heavy precipitation (over SAF).

3.4 Impacts of stratospheric aerosol injection on wet and dry spells

As for Figures 7 and 8 presents changes in the maximum length of consecutive wet days [CWD; Figure 8(a)–8(d)], the highest precipitation amount in 5 consecutive days [RX5day; Figure 8(r)–8(h)] and in the maximum length of consecutive dry days [CDD; Figure 8(i)–8(l)].

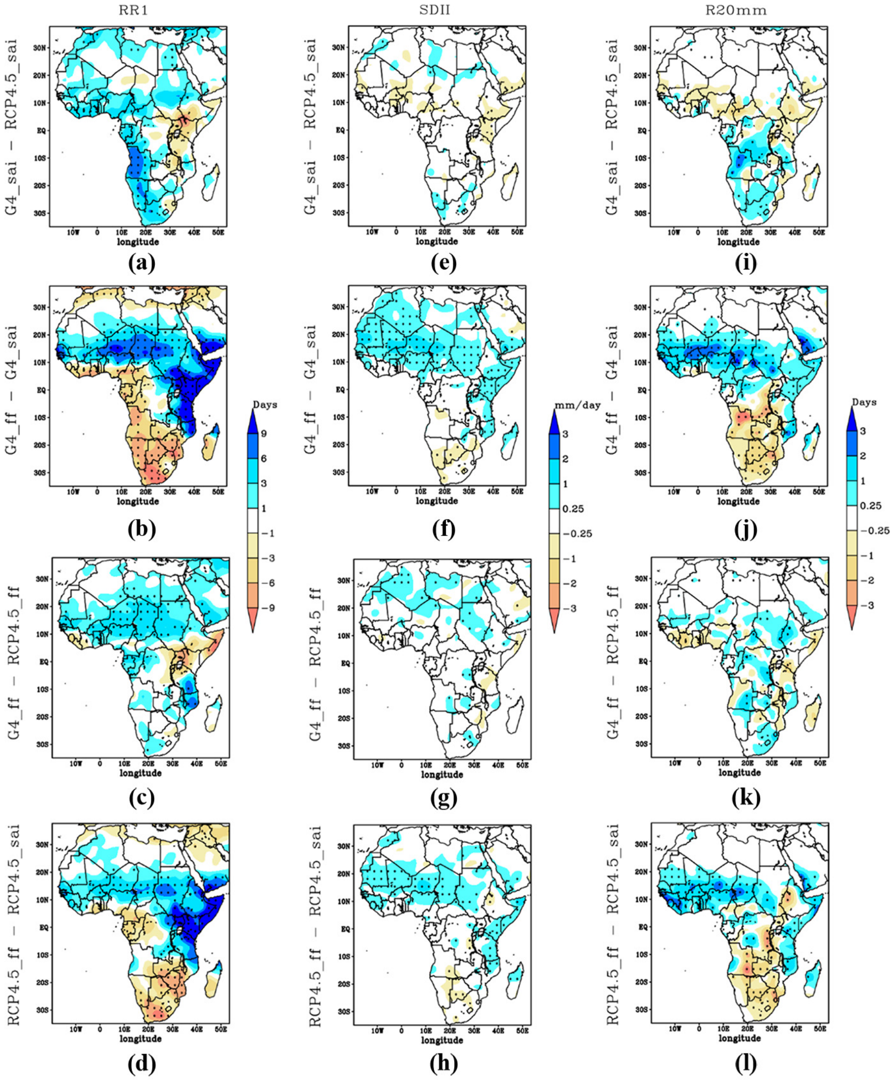

Notes: NB: Black dots on the maps delimit areas with significant changes at 95% confidence level, SAI period refers to 2030–2050 and ff to 2070–2090. The first row of Figure 7(a), 7(e) and 7(i) compares the G4 to RCP4.5 experiment during the injection period (near future, 2030-2050). The second row of Figure 7(b), 7(f) and 7(j) compares changes in precipitation indices between the far future (after the injection period or 2070–2090) and during the injection period (2030–2050) of the G4 experiment. The third row of Figure 7(c), 7(g) and 7(k) compares during the far future the changes between G4 andRCP4.5 after the injection period. Finally, the fourth raw of Figure 7(d), 7(h) and 7(l) shows the difference between far and near futures of the RCP4.5 experiment

Figure 7.
Changes of precipitation indices RR1 (first column), SDII (second column) and R20mm (third column)

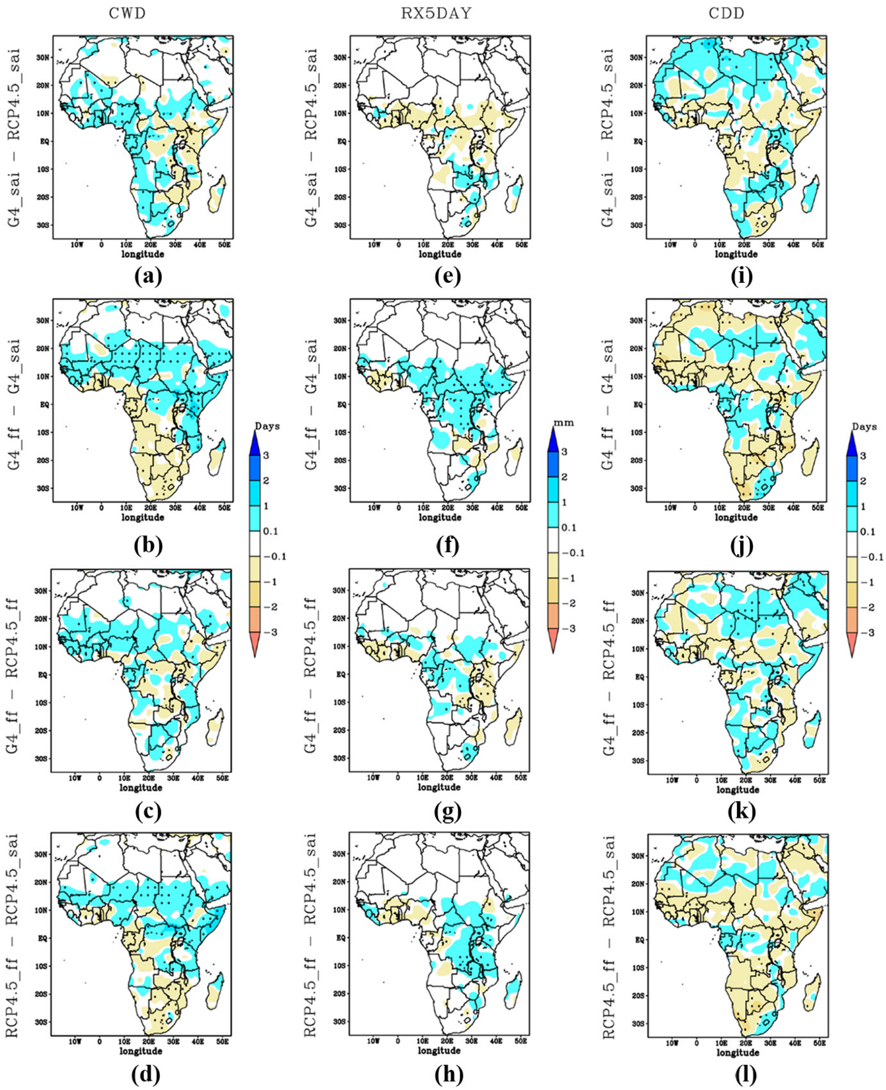

Notes: NB: Black dots on the maps delimit areas with significant changes at 95% confidence level, SAI period refers to 2030–2050 and ff to 2070–2090. The first row of Figure 8(a), 8(e) and 8(i) compares the G4 to RCP4.5 experiment during the injection period (near future, 2030–2050). The second row of Figure 8(b), 8(f) and 8(j) compares changes in precipitation indices between the far future (after the injection period or 2070–2090) and during the injection period (2030–2050) of the G4 experiment. The third row of Figure 8(c), 8(g) and 8(k) compares during the far future the changes between G4 andRCP4.5 after the injection period. Finally, the fourth raw of Figure 8(d), 8(h) and 8(l) shows the difference between far and near futures of the RCP4.5 experiment

Figure 8.
Effects of SAI during injection and stoppage on CWD (first column), RX5DAY (second column) and CDD (third column)

Generally, during the injection period, there is no significant change between G4 and RCP4.5 in the number of CWDs in a large part of the continent [Figure 8(a)]. The wet spells tend to last longer in the WAF region and along the Western side of SAF [Figure 8(a)] in G4 than in RCP4.5 simulations and to shorten in EAF over the Great Lakes region and Eastern part of SAF. The termination effect will lead to a significant increase of CWD in the whole tropical band except the Guinea Coast of WAF and a decrease of CWD over SAF [Figure 8(b)]. Generally, compared to CWD projected in RCP4.5 [Figure 8(c)], CWD due to the termination effect will last longer over WAF and in several parts of SAF, suggesting that the shortening of wet spells projected under RCP4.5 over SAF will be mitigated by the termination effect [Figure 8(d)].

Figure 8(e) shows that during the injection period, there is no significant change between G4 and RCP4.5 in the maximum precipitation in five consecutive days (Rx5day) in the whole continent. Rx5day tends to be weaker over the tropics (WAF and EAF) in G4 than in RCP4.5 simulations and to be slightly greater in the Eastern side of SAF. The termination effect will lead to an increase of Rx5day in the tropical band with significant values in Central Africa except for the Guinea Highlands of WAF and over the Eastern side of SAF [Figure 8(f)]. Generally, compared to Rx5day projected in RCP4.5 [Figure 8(g)], Rx5day due to the termination effect will be greater in Central Africa and weaker over EAF, suggesting that the termination effect will decrease the maximum of precipitation in 5 consecutive days, contributing to mitigating the risk of the flood ([Figure 8(g), 8(h)].

SAI might contribute to mitigating drought spots projected in RCP4.5 and RCP8.5 (Diedhiou *et al.*, 2018) over SAF and the Western side of WAF. Rx5day [Figure 7(e)] does not significantly change in G4 compared to RCP4.5, except over the tropics where a significant decrease is noted during the injection period, in agreement with a decrease of convective activity in the ITCZ. Dry spells last significantly longer over NAF [Figure 7(i)] in G4 than in RCP4.5 and decrease significantly over EAF. As Figure 6(a) showed previously that total annual rainfall will increase in NAF due to SAI and Figure 7(i) reveals that dry spells will last longer in the same region, the increase of precipitation in NAF may be caused either by an increase in the number of rainy days or of the intensity of rainfall or the occurrence of heavy rainfall.

Figure 8(i) shows that during the injection period, there is no significant change between G4 and RCP4.5 in the maximum length of consecutive dry days (CDD) in the whole continent except over NAF where a significant increase in CCD is noted. The length of dry spells tends to be slightly weaker over the tropics (WAF and EAF) in G4 than in RCP4.5 simulations and to be slightly greater in the Western side of WAF and over the Western and Northern sides of SAF. The termination effect will lead to a decrease of CDD in large parts of the continent except for Central Africa in WAF and Sothern part of NAF [Figure 8(j)]. Generally, compared to CDD projected in RCP4.5 [Figure 8(k)], CDD due to the termination effect will last longer in large parts of extratropical regions but the changes are not significant [Figure 8(k), 8(l)].

4. General discussion

Three Coupled Model Intercomparison Project Phase 5 models involved in the G4 experiment of the GeoMIP project were used to investigate the impact of SAI and its termination effect on the mean surface air temperature and precipitation extremes in four regions of Africa. During SAI, the air temperature continues warming but at a lower rate compared to RCP4.5 in agreement with previous studies (Yu *et al.*, 2015; Pinto *et al.*, 2020). Indeed, Pinto *et al.* (2020) found using Stratospheric Aerosol Geoengineering Large Ensemble (GLENS) compared to the RCP8.5 scenario that SRM significantly reduces temperature means in the African continent. The analysis of G4-experiment simulations over Africa as performed in our study reveals that the expected temperature will be lower than in RCP4.5 (known to be cooler than RCP8.5), confirming that SAI can indeed offset some of the effects of climate change.

However, temperature changes associated with the termination effect are not only explained by the amount of SAI in force, but also by land and ocean carbon uptake potential. Indeed, it was reported that only 45% of total carbon emitted from anthropogenic activities stayed in the atmosphere for a few decades and the remainder is up taken in carbon reservoirs in the ocean and land (Le Quéré 2010). It has been proved that 20 years after stopping SRM, there is a release in average 8 ± 11 GtC of the carbon previously removed out of the atmosphere attributed to the land biosphere (Plazzotta *et al.*, 2019) which could affect the climate variables. There is a long-lasting response after termination that is somewhat unexpected because it is not due to radiative forcing but feedbacks such as land surface albedo and carbon storage. The authors suppose that the albedo change is more important than the carbon storage over land as found by Cheng *et al.* (2017). Hence, after the SAI period, the G4-experiment temperature will sharply rise to resemble the non-geo-engineering scenario (RCP4.5) (Kashimura *et al.*, 2017; Lee *et al.*, 2019). This explains why during the injection period the continental temperature will continue to rise but at a lower rate in G4 than under RCP4.5 simulation. After the injection period, the surface air temperature will continue to increase in G4 over the period 2070–2090 but at a higher rate than during the injection.

The G4-experiment shows that SAI and its termination will substantially affect precipitation over the entire continent, but the impact varies according to the region. During SAI, the model ensemble mean exhibits a significant increase in total precipitation over extratropical zones (NAF and SAF) with a greater increase in SAF (20–80 mm/year and above over the Western side) while a reduction is promised over the tropical band with the greatest value in EAF (20–80 mm/year shift over the Great Lake subregions). This result is in agreement with the study of Wei *et al.* (2018) using the G4 experiment and highlighting that over the tropics, especially over Africa and South Asia, there is a large reduction in precipitation up to 37.1 and 52.3 mm per year while an increase is noted over the extratropical band (over NAF and significant over SAF) over 2030–2069 relative to 1960–1999. Haywood *et al.* (2013) found in G3 and G4 experiments using uniform SAI that there is a small increase in precipitation ranging from 0–50 mm/year over Western and Southern subregions of NAF. Trisos *et al.* (2018) found that either overland or over the ocean, the G4 scenario predicted lower temperature and precipitation than the RCP4.5 scenario during SAI deployment.

The authors suggest that the decrease of precipitation in the tropical band (WAF and EAF) could be due to a change in Hadley cell circulation intensity, mainly in the weakening of the upward motion over the tropical band caused by cooling in surface air temperature associated with a decrease of downward solar radiation due to SAI. Indeed, Schmidt *et al.* (2012) and Smyth *et al.* (2017) attributed the decrease of precipitation under the G1 experiment to a shift of latitudinal seasonal amplitude of ITCZ, and Guo *et al.* (2018) related it to a reduction in the intensity of the Hadley circulation.

After the injection, the termination effect leads to a significant decrease of the total precipitation over SAF, over the Guinea Coast of WAF and coastal NAF, while a significant increase of precipitation is noted over the tropical band (WAF and EAF) and the Eastern SAF. Pinto *et al.* (2020) also found out that under SRM forcing using the GLENS ensemble, total precipitation is projected to decrease in many parts of SAF, CAF and WAF relative to the historical period. Indeed, after the injection period, most regions are projected to recover from the decline of precipitation especially tropical regions (WAF and EAF).

When comparing G4 runs to the RCP4.5 (no SAI), the termination effect of SAI is projected to significantly increase the total precipitation in large parts of Africa, especially over Central Sahel, except in EAF (over the Great Lake and Horn of Africa subregions) and the Guinean Highlands in WAF. The Sahara Desert will become significantly wetter and this may open new opportunities in the development of the region, but this needs to be investigated further. The rainfall deficit over SAF projected under RCP4.5 (without SAI) will be mitigated by the termination effect of SAI, while the significant strong increase of rainfall over Central Sahel will enhance the risk of floods in the Sahel.

During the injection period, the decrease of total precipitation in the tropics is associated with an increase of RR1 and a reduction of SDII while the increase of precipitation over the western side of SAF is associated with an increase of RR1, of R20mm and of CWD. The slight increase of precipitation over NAF seems to be associated with an increase of RR1. During SAI, the decrease of precipitation over the tropical band was also associated with a decrease in evaporation and net evaporation as well as of runoff (which is significant over EAF) while the contrasting effect was noted over the extratropical band especially over SAF (Wei *et al.*, 2018). Moreover, the decrease in the highest precipitation amount in 5 consecutive days and CDD over the tropical band (WAF and EAF) is in agreement with the study of Ji *et al.* (2018) during the injection period.

Compared to RCP4.5, the termination of SAI after G4 will lead to a significant increase of RR1 and CWD in the tropics with maxima over Central Sahel and the Sahara Desert, of RR1 and R20mm over SAF and of RR1 and SDII over NAF. Over EAF, the termination effect is projected to induce a deficit of rainfall compared to RCP4.5 over the Great Lake and Horn of Africa subregions. Thus, after the injection period, the risk of floods projected under RCP8.5 of CORDEX will be exacerbated under G4 termination and the projection of a likely increase of dry spells [WAF, Diedhiou *et al.* (2018), Klutse *et al.* (2018) and EAF, Osima *et al.* (2018)] is noted to be reduced by SAI due to an increase of the length of wet spells of numbers of rainy and very heavy precipitation days especially in the Sahelian band. However, (Wei *et al.*, 2018) found that in general, the G4 return periods of the flood (over 2030–2069) are less changed from the historical levels than under RCP4.5. Over EAF, a significant decrease in total precipitation is mainly due to a decrease in the number of rainy days and of days with heavy precipitation and the rainfall intensity. Then, the SAI could mitigate the risk of flood due to an increase in the number of wet days and very heavy precipitation days (under RCP4.5 simulation). The projection of a likely increase of dry spells in Central Africa under RCP8.5 of the CORDEX by Mba *et al.* (2018) would be mitigated by the SAI due to an increase in total precipitation associated with an increase of the number of rainy and very heavy precipitation days as well as the length of wet spells and the Rx5day. Likewise, over the extratropical band especially over SAF, the projected increase in a dry spell by Maure *et al.* (2018) under the RCP8.5 experiment of the CORDEX will be mitigated by the increase of the number of rainy and very heavy precipitation days and rainfall intensity. Therefore, after the injection, the SAI may mitigate the water scarcity in the SAF region where water availability is a challenge. NAF will experience more rainfall (total precipitation, number of rainy days and rainfall intensity) with G4 geoengineering, but as dry spells will last longer, there might be a high risk of flooding in this subregion.

However, the potential impacts on precipitation indices vary from one model to another and the inter-model variation in both the amplitude and direction of change may be attributed to insufficiencies in the ability of global climate models to resolve convective rainfall (Roehrig *et al.*, 2013; Klutse *et al.*, 2015). This confirms the unequal responses according to the region and the model to the radiative forcing geoengineering method (Park *et al.*, 2019).

5. Conclusion

The SAI under G4-experiment simulations over Africa is found to significantly reduce the expected temperature under RCP4.5 (known to be cooler than RCP8.5) which then confirms that SAI can indeed offset some of the effects of global warming. It is important to note that during the injection period, the continental temperature will continue to rise but at a lower rate in G4 than under RCP4.5 simulation. After the injection period, the surface air temperature will continue to rise in G4 that means that the warming over the period 2070–2090 will be higher than during the injection period (2020–2069). However, the continent will be less warm in G4 than projected under RCP4.5.

The total precipitation was noted to considerably decrease during the injection period in the tropical band (WAF and EAF, with greatest reduction in EAF) associated with an increase of RR1 and a reduction of SDII during the SAI. This may be associated with risk of occurrence of drought that might affect the water availability for all water-consumed sectors, namely, water demand and supply, agriculture, health, security, economy as well as energy especially hydroelectricity generation.

A significant increase in total precipitation is noted during injection over extratropical zones (NAF associated with an increase of RR1 and SAF associated with an increase of RR1, of R20mm and of CWD) with a greater increase in SAF and with a risk of flooding and negative socio-economic impacts.

The halting of the injection may leads to a significant decrease of the total precipitation over SAF, over the Guinea Coast of WAF and coastal NAF associated with a significant increase over the tropical band (WAF and EAF) and the Eastern SAF due to the termination.

Overall, the change vary according to the region and the phase of the project (SAI or PostSAI). Therefore, a deep analysis on the implication of G4-experiment with regional climate models or with advanced statistical methods should be done in each African subregion by correcting the bias of the data set and their effects on the hydrological cycle, water resources availability, agriculture and energy production should be assessed. Further investigation is also needed to understand the implication of SAI on West Africa rainfall characteristics, namely, monsoon, Africa Easterly Jet and Tropical Easterly Jet as well as on extremes temperature. Considering that rain-fed agriculture accounts for a large part of African economies, further investigations are needed to understand the impacts of such SAI geoengineering on key sectors such as water resources, agriculture and energy in each African subregion to guide the adaptation and mitigation policies.

References

Arora, V.K., Scinocca, J.F., Boer, G.J., Christian, J.R., Denman, K.L., Flato, G.M., … Merryfield, W.J. (2011), "Carbon emission limits required to satisfy future representative concentration pathways of greenhouse gases", *Geophysical Research Letters*, Vol. 38 No. 5, pp. 3-8, doi: 10.1029/2010GL046270.

Brown, O. and Crawford, A. (2008a), "Climate change: a new threat to stability in West Africa? Evidence from Ghana and Burkina Faso", *African Security Studies*, available at: www.tandfonline.com/doi/pdf/10.1080/10246029.2008.9627482

Brown, Oli,. and Crawford, A. (2008b), "Assessing the security implications of climate change for West Africa: country case studies of Ghana and Burkina Faso", *International Institute for Sustainable Development*, available at: www.iisd.org/pdf/2008/security_implications_west_africa.pdf

Budyko, M.I. (1977), *Climatic Changes*, Vol. 261, *American Geophysical Union*, Washington, DC.

Burke, M.B., Miguel, E., Satyanath, S., Dykema, J.A. and Lobell, D.B. (2009), "Warming increases the risk of civil war in africa", *Proceedings of the National Academy of Sciences*, Vol. 106 No. 49, pp. 20670-20674, doi: 10.1073/pnas.0907998106.

Cheng, W., Moore, J.C., Cao, L., Ji, D. and Zhao, L. (2017), "Simulated climate effects of desert irrigation geoengineering", *Scientific Reports*, Vol. 7 No. 1, pp. 1-10, doi: 10.1038/srep46443.

Chin-Yee, S. (2016), "Africa and the paris climate change agreement", *African Affairs*, Vol. 115 No. 459, pp. 359-368, doi: 10.1093/afraf/adw005.

Collins, J.M. (2011), "Temperature variability over africa", *Journal of Climate*, Vol. 24 No. 14, pp. 3649-3666, doi: 10.1175/2011JCLI3753.1.

Crutzen, P.J. (2006), "Albedo enhancement by stratospheric Sulfur injections: a contribution to resolve a policy dilemma? ", *Climatic Change*, Vol. 77 Nos 3/4, pp. 211-220, doi: 10.1007/s10584-006-9101-y.

Di Baldassarre, G., Montanari, A., Lins, H., Koutsoyiannis, D., Brandimarte, L. and Blschl, G. (2010), "Flood fatalities in Africa: from diagnosis to mitigation", *Geophysical Research Letters*, Vol. 37 No. 22, pp. 2-6, doi: 10.1029/2010GL045467.

Diedhiou, A., Bichet, A., Wartenburger, R., Seneviratne, S.I., Rowell, D.P., Sylla, M.B., … Affholder, F. (2018), "Changes in climate extremes over west and Central Africa at 1.5°C and 2°C global warming", *Environmental Research Letters*, Vol. 13 No. 6, doi: 10.1088/1748-9326/aac3e5.

Donat, M.G., Sillmann, J., and Fischer, E.M. (2020), "Changes in climate extremes in observations and climate model simulations. From the past to the future", *Climate Extremes and Their Implications for Impact and Risk Assessment*, doi: 10.1016/b978-0-12-814895-2.00003-3

Du, W., Fitzgerald, G.J., Clark, M. and Hou, X.Y. (2010), "Health impacts of floods", *Prehospital and Disaster Medicine*, Vol. 25 No. 3, pp. 265-272, doi: 10.1017/S1049023X00008141.

Ferraro, A.J., Charlton-Perez, A.J. and Highwood, E.J. (2014), "A risk-based framework for assessing the effectiveness of stratospheric aerosol geoengineering", *PLoS ONE*, Vol. 9 No. 2, doi: 10.1371/journal.pone.0088849.

Ferraro, A.J. and Griffiths, H.G. (2016), "Quantifying the temperature-independent effect of stratospheric aerosol geoengineering on global-mean precipitation in a multi-model ensemble", *Environmental Research Letters*, Vol. 11 No. 3, doi: 10.1088/1748-9326/11/3/034012.

Ferraro, A.J., Highwood, E.J. and Charlton-Perez, A.J. (2014), "Weakened tropical circulation and reduced precipitation in response to geoengineering", *Environmental Research Letters*, Vol. 9 No. 1, doi: 10.1088/1748-9326/9/1/014001.

Gannon, K.E., Conway, D., Pardoe, J., Ndiyoi, M., Batisani, N., Odada, E. and Siderius, C. (2018), "Business experience of floods and drought-related water and electricity supply disruption in three cities in Sub-Saharan Africa during the 2015/2016 El Niño", *Global Sustainability*, Vol. 1, doi: 10.1017/sus.2018.14.

Gebremeskel, G., Tang, Q., Sun, S., Huang, Z., Zhang, X. and Liu, X. (2019), "Droughts in east africa: Causes, impacts and resilience", *Earth-Science Reviews*, Vol. 193 (April), pp. 146-161, doi: 10.1016/j.earscirev.2019.04.015.

Gebremeskel Haile, G., Tang, Q., Leng, G., Jia, G., Wang, J., Cai, D. and Zhang, Q. (2020), "Long-term spatiotemporal variation of drought patterns over the greater horn of Africa", *Science of the Total Environment*, Vol. 704, doi: 10.1016/j.scitotenv.2019.135299.

Giorgi, F. and Francisco, R. (2000), "Uncertainties in regional climate change prediction: a regional analysis of ensemble simulations with the HADCM2 coupled AOGCM", *Climate Dynamics*, Vol. 16 Nos 2/3, pp. 169-182, doi: 10.1007/PL00013733.

Guo, A., Moore, J.C. and Ji, D. (2018), "Tropical atmospheric circulation response to the G1 sunshade geoengineering radiative forcing experiment", *Atmospheric Chemistry and Physics*, Vol. 18 No. 12, pp. 8689-8706.

Hartmann, D.L. Klein Tank, A.M.G. Rusticucci, M. Alexander, L.V. Brönnimann, S. Charabi, Y.A.R. … Zhai, P. (2013), "Observations: atmosphere and surface", Climate Change 2013 the Physical Science Basis: Working Group I Contribution to the Fifth Assessment Report of the Intergovernmental Panel on Climate Change (Vol. 9781107057), doi: 10.1017/CBO9781107415324.008

Haywood, J.M., Jones, A., Bellouin, N. and Stephenson, D. (2013), "Asymmetric forcing from stratospheric aerosols impacts Sahelian rainfall", *Nature Climate Change*, Vol. 3 No. 7, pp. 660-665, doi: 10.1038/nclimate1857.

Herring, S.C., Hoerling, M.P., Peterson, T.C. and Stott, P.A. (2014), "Explaining extreme events of 2013 from a climate perspective", *Bulletin of the American Meteorological Society*, Vol. 95 No. 9, pp. S1-S96.

Janssen, A. (2005), "Resampling student's t-type statistics", *Annals of the Institute of Statistical Mathematics*, Vol. 57 No. 3, pp. 507-529, doi: 10.1007/BF02509237.

Ji, D., Fang, S., Curry, C.L., Kashimura, H., Watanabe, S. and Cole, J.N.S. (2018), "Extreme temperature and precipitation response to solar dimming and stratospheric aerosol geoengineering", *Atmospheric Chemistry and Physics*, Vol. 18 No. 14, pp. 10133-10156.

Kashimura, H., Abe, M., Watanabe, S., Sekiya, T., Ji, D. and Moore, J.C. (2017), "Shortwave radiative forcing, rapid adjustment, and feedback to the surface by sulfate geoengineering: analysis of the geoengineering model intercomparison project G4 scenario", *Atmospheric Chemistry and Physics*, Vol. 17 No. 5, pp. 3339-3356, doi: 10.5194/acp-17-3339-2017.

Kattsov, V., Federation, R., Reason, C., Africa, S., Uk, A.A., Uk, T.A., … Uk, A.S. (2013), "Evaluation of climate models 9", in Stocker, T.F., Qin, D. Plattner, G.-K. Tignor, M. Allen, S.K. Boschung, J. Nauels, A. and Xia Y. (Ed.), *Climate Change 2013: The Physical Science Basis. Contribution of Working Group I to the Fifth Assess- Ment Report of the Intergovernmental Panel on Climate Change*, Cambridge University Press, Cambridge, and New York, NY, pp. 741-866.

Kitous, A. and Keramidas, K. (2015), "Analysis of scenarios integrating the INDCs", JRC POLICY BRIEF, pp. 1-11, available at: https://ec.europa.eu/jrc/en/news/current-climate-commitments-would-increase-global-temperature-around-3-degrees

Klein Tank, A.M.G. Zwiers, F.W. and Zhang, X. (2009), "Guidelines on extremes guidelines on analysis of extremes in a changing climate in support of informed decisions", Climate Data and Monitoring, Retrieved from File Attachment.

Kleinschmitt, C., Boucher, O. and Platt, U. (2018), "Sensitivity of the radiative forcing by stratospheric sulfur geoengineering to the amount and strategy of the SO2injection studied with the LMDZ-S3A model", *Atmospheric Chemistry and Physics*, Vol. 18 No. 4, pp. 2769-2786, doi: 10.5194/acp-18-2769-2018.

Klutse, N.A.B., Ajayi, V.O., Gbobaniyi, E.O., Egbebiyi, T.S., Kouadio, K., Nkrumah, F., … Dosio, A. (2018), "Potential impact of 1.5°C and 2°C global warming on consecutive dry and wet days over West Africa", *Environmental Research Letters*, Vol. 13 No. 5, doi: 10.1088/1748-9326/aab37b.

Klutse, N.A.B., Sylla, M.B., Sarr, I.D., A., Büchner, A.D., Diedhiou, A., Matthias, A.K., Panitz, H.-J. … (2015), "Daily characteristics of west African summer monsoon precipitation in Cordex simulations", *Theoretical and Applied Climatology*, Vol. 123 Nos 1/2, pp. 369-386, doi: 10.1007/s00704-014-1352-3.

Kogan, F., Guo, W. and Yang, W. (2019), "Drought and food security prediction from NOAA new generation of operational satellites", *Geomatics, Natural Hazards and Risk*, Vol. 10 No. 1, pp. 651-666, doi: 10.1080/19475705.2018.1541257.

Kravitz, B., Robock, A., Boucher, O., Schmidt, H., Taylor, K.E., Stenchikov, G. and Schulz, M. (2011), "The geoengineering model intercomparison project (GeoMIP)", *Atmospheric Science Letters*, Vol. 12 No. 2, pp. 162-167, doi: 10.1002/asl.316.

Le Quéré, C. (2010), "Trends in the land and ocean carbon uptake", *Current Opinion in Environmental Sustainability*, Vol. 2 No. 4, pp. 219-224, doi: 10.1016/j.cosust.2010.06.003.

Lee, H., Ekici, A., Tjiputra, J., Muri, H., Lawrence, D.M. and Schwinger, J. (2019), "The response of permafrost and high – latitude ecosystems under large – scale stratospheric aerosol injection and its termination", *Earth's Future*, Vol. 7 No. 6, pp. 605-614, doi: 10.1029/2018EF001146.

Lima, M.I.P., De, Santo, F.E., Ramos, A.M. and Trigo, R.M. (2014), "Trends and correlations in annual extreme precipitation indices for mainland Portugal, 1941 – 2007", *Theoretical and Applied Climatology*, Vol. 119 Nos 1/2, pp. 55-75, doi: 10.1007/s00704-013-1079-6.

Lydersen, S. (2015), "Statistical review: frequently given comments", *Annals of the Rheumatic Diseases*, Vol. 74 No. 2, pp. 323-325, doi: 10.1136/annrheumdis-2014-206186.

Maure, G., Pinto, I., Ndebele-Murisa, M., Muthige, M., Lennard, C., Nikulin, G. and Meque, A. (2018), "The Southern African climate under 1.5°C and 2°C of global warming as simulated by CORDEX regional climate models", *Environmental Research Letters*, Vol. 13 No. 6, doi: 10.1088/1748-9326/aab190.

Mba, W.P., Longandjo, G.N.T., Moufouma-Okia, W., Bell, J.P., James, R., Vondou, D.A., … Dosio, A. (2018), "Consequences of 1.5°C and 2°C global warming levels for temperature and precipitation changes over Central Africa", *Environmental Research Letters*, Vol. 13 No. 5, doi: 10.1088/1748-9326/aab048.

Mideksa, T.K. and Kallbekken, S. (2010), "The impact of climate change on the electricity market : a review", *Energy Policy*, Vol. 38 No. 7, pp. 3579-3585, doi: 10.1016/j.enpol.2010.02.035.

Ndiaye, A., Adamou, R., Gueye, M. and Diedhiou, A. (2017), "Global warming and heat waves in West-Africa: impacts on electricity consumption in Dakar (Senegal) and Niamey (Niger)", *International Journal of Energy and Environmental Science*, Vol. 2 No. 1, pp. 16-26, doi: 10.11648/j.ijees.20170201.13.

Nikulin, G., Lennard, C., Dosio, A., Kjellström, E., Chen, Y., Hansler, A. and Somot, S. (2018), "The effects of 1.5 and 2 degrees of global warming on Africa in the CORDEX ensemble", *Environmental Research Letters*, Vol. 13 No. 6, doi: 10.1088/1748-9326/aab1b1.

Orimoloye, I.R., Ololade, O.O., Mazinyo, S.P., Kalumba, A.M., Ekundayo, O.Y., Busayo, E.T., … Nel, W. (2019), "Spatial assessment of drought severity in cape town area, South Africa", *Heliyon*, Vol. 5 No. 7, p. e02148, doi: 10.1016/j.heliyon.2019.e02148.

Osima, S., Indasi, V.S., Zaroug, M., Endris, H.S., Gudoshava, M., Misiani, H.O., … Dosio, A. (2018), "Projected climate over the greater horn of Africa under 1.5°C and 2°C global warming", *Environmental Research Letters*, Vol. 13 No. 6, doi: 10.1088/1748-9326/aaba1b.

Paeth, H., Hall, N.M.J., Gaertner, M.A., Alonso, M.D., Moumouni, S., Polcher, J., … Rummukainen, M. (2011), "Progress in regional downscaling of west African precipitation", *Atmospheric Science Letters*, Vol. 12 No. 1, pp. 75-82, doi: 10.1002/asl.306.

Park, C.E., Jeong, S.J., Fan, Y., Tjiputra, J., Muri, H. and Zheng, C. (2019), "Inequal responses of drylands to radiative forcing geoengineering methods", *Geophysical Research Letters*, Vol. 46 No. 23, pp. 14011-14020, doi: 10.1029/2019GL084210.

Parkes, B., Defrance, D., Sultan, B., Ciais, P. and Wang, X. (2018), "Projected changes in crop yield mean and variability over West Africa in a world 1.5K warmer than the pre-industrial era", *Earth System Dynamics*, Vol. 9 No. 1, pp. 119-134, doi: 10.5194/esd-9-119-2018.

Peterson, T.C. Folland, C. Gruza, G. Hogg, W. Mokssit, A. and Plummer, N. (2001), "Report on the activities of the working group on climate change detection and related rapporteurs 1998-2001".

Pinto, I., Jack, C., Lennard, C., Tilmes, S. and Odoulami, R.C. (2020), "Africa's climate response to solar radiation management with stratospheric aerosol", *Geophysical Research Letters*, Vol. 47 No. 2, pp. 1-10, doi: 10.1029/2019GL086047.

Plazzotta, M., Séférian, R. and Douville, H. (2019), "Impact of solar radiation modifi cation on allowable CO 2 emissions: what can We learn from multimodel simulations ?", *Earth's Future*, Vol. 7 No. 6, pp. 664-676, doi: 10.1029/2019EF001165.

Rahm, D. (2018), "Geoengineering climate change solutions: public policy issues for national and global governance", *Humanities AndSocial Sciences Review*, Vol. 8 No. 2, pp. 139-148.

Robock, A. (2000), "Ic eruptions", *Reviews of Geophysics*, Vol. 38 No. 2, pp. 191-219.

Roehrig, R., Bouniol, D., Guichard, F., Hourdin, F., Déric. and Redelsperger, J.L. (2013), "The present and future of the West African monsoon: a process-oriented assessment of CMIP5 simulations along the AMMA transect", *Journal of Climate*, Vol. 26 No. 17, pp. 6471-6505, doi: 10.1175/JCLI-D-12-00505.1.

Roudier, P., Sultan, B., Quirion, P. and Berg, A. (2011), "The impact of future climate change on West African crop yields: what does the recent literature say?", *Global Environmental Change*, Vol. 21 No. 3, pp. 1073-1083, doi: 10.1016/j.gloenvcha.2011.04.007.

Schmidt, H., Alterskjær, K., Bou Karam, D., Boucher, O., Jones, A., Kristjánsson, J.E. and Timmreck, C. (2012), "Solar irradiance reduction to counteract radiative forcing from a quadrupling of CO 2: climate responses simulated by four earth system models", *Earth System Dynamics*, Vol. 3 No. 1, pp. 63-78, doi: 10.5194/esd-3-63-2012.

Seneviratne, S.I., Nicholls, N., Easterling, D., Goodess, C.M., Kanae, S., Kossin, J., Zwiers, F.W., A.P.M. M. (2012), "Changes in climate extremes and their impacts on the natural physical environment", in Field, M. T. Barros, C.B., V. Stocker, T.F. Qin, D. Dokken, D.J. Ebi, K.L. Mastrandrea, M.D. Mach, K.J.,G.-KSK. (Eds), *Managing the Risks of Extreme Events and Disasters to Advance Climate Change Adaptation: Special Report of the Intergovernmental Panel on Climate Change*, Vol. 9781107025, pp. 109-230, doi: 10.1017/CBO9781139177245.006

Sillmann, J. and Roeckner, E. (2008), "Indices for extreme events in projections of anthropogenic climate change", *Climatic Change*, Vol. 86 Nos 1/2, pp. 83-104, doi: 10.1007/s10584-007-9308-6.

Smyth, J.E., Russotto, R.D. and Storelvmo, T. (2017), "Thermodynamic and dynamic responses of the hydrological cycle to solar dimming", *Atmospheric Chemistry and Physics*, Vol. 17 No. 10, pp. 6439-6453, doi: 10.5194/acp-17-6439-2017.

Sönke, K. Eckstein, D. Dorsch, L. and Fischer, L. (2015), "Global climate risk index 2016: Who suffers most from extreme weather events? Weather-related loss events in 2014 and 1995 to 2014", Available at: https://doi.org/978-3-943704-04-4

Sylla, M.B., Nikiema, P.M., Peter Gibba, I., bourahima, K., and Klutse, N.A.B. (2016), And "Climate change over west africa: Recent trends and future projections", in Hesselberg JAYJ. (Eds), *Adaptation to Climate Change and Variability in Rural West Africa*, Springer, pp. 25-40, 10.1007/978-3-319-31499-0_3

Thomas-Hope, E. (2018), "Book review: Book review", *Journal of Early Childhood Research*, Vol. 40, pp. 223-225, doi: 10.1177/1476718x11406241.

Trenberth, K.E., Fasullo, J.T. and Shepherd, T.G. (2015), "Attribution of climate extreme events", *Nature Climate Change*, Vol. 5 No. 8, pp. 725-730, doi: 10.1038/nclimate2657.

Trisos, C.H., Amatulli, G., Gurevitch, J., Robock, A., Xia, L. and Zambri, B. (2018), "For biodiversity of solar geoengineering implementation and termination", *Nature Ecology & Evolution*, doi: 10.1038/s41559-017-0431-0.

Visioni, D., Pitari, G., Aquila, V., Goddard, N. and Flight, S. (2017), "Sulfate geoengineering : a review of the factors controlling the needed injection of Sulfur Dioxide", *Atmospheric Chemistry and Physics*, Vol. 17 No. 6, pp. 3879-3889, doi: 10.5194/acp-17-3879-2017.

Von Uexkull, N. (2014), "Sustained drought, vulnerability and civil conflict in Sub-Saharan Africa", *Political Geography*, Vol. 43, pp. 16-26, doi: 10.1016/j.polgeo.2014.10.003.

Waha, K., Krummenauer, L., Adams, S., Aich, V., Baarsch, F., Coumou, D. and Schleussner, C.F. (2017), "Climate change impacts in the Middle east and Northern Africa (MENA) region and their implications for vulnerable population groups", *Regional Environmental Change*, Vol. 17 No. 6, pp. 1623-1638, doi: 10.1007/s10113-017-1144-2.

Watanabe, S., Hajima, T., Sudo, K., Nagashima, T., Takemura, T., Okajima, H. and Kawamiya, M. (2011), "MIROC-ESM 2010: Model description and basic results of CMIP5-20c3m experiments", *Geoscientific Model Development*, Vol. 4 No. 4, pp. 845-872, doi: 10.5194/gmd-4-845-2011.

Weber, T., Haensler, A., Rechid, D., Pfeifer, S., Eggert, B. and Jacob, D. (2018), "Analyzing regional climate change in Africa in a 1.5, 2, and 3°C global warming world", *Earth's Future*, Vol. 6 No. 4, pp. 643-655, doi: 10.1002/2017EF000714.

Wei, L. Ji, D. Miao, C. Muri, H. and Moore, J.C. (2018), "Global streamflow and flood response to stratospheric aerosol geoengineering", pp. 16033-16050.

World Meteorological Organization (2018), "Guidelines on the defintion and monitoring of extreme weather and climate events", *Task Team on the Definition of Extreme Weather and Climate Events* (December 2015), p. 62, doi: 10.1109/CSCI.2015.171.

Yu, X., Moore, J.C., Cui, X., Rinke, A., Ji, D., Kravitz, B. and Yoon, J.H. (2015), "Impacts, effectiveness and regional inequalities of the GeoMIP G1 to G4 solar radiation management scenarios", *Global and Planetary Change*, Vol. 129, pp. 10-22, doi: 10.1016/j.gloplacha.2015.02.010.

Zhang, X., Alexander, L., Hegerl, G.C., Jones, P., Tank, A.K., Peterson, T.C. and Zwiers, F.W. (2011), "Indices for monitoring changes in extremes based on daily temperature and precipitation data", *Wiley Interdisciplinary Reviews: Climate Chang*, Vol. 2 No. 6, pp. 851-870, doi: 10.1002/wcc.147.

Further reading

Intergovernmental Panel on Climate Change (IPCC) (2013), "Technical summary", *Climate Change 2013: The Physical Science Basis. Contribution of Working Group I to the Fifth Assessment Report of the Intergovernmental Panel on Climate Change*. Cambridge University Press, Cambridge, and New York, NY, https://www.ipcc.ch/.

Appendix

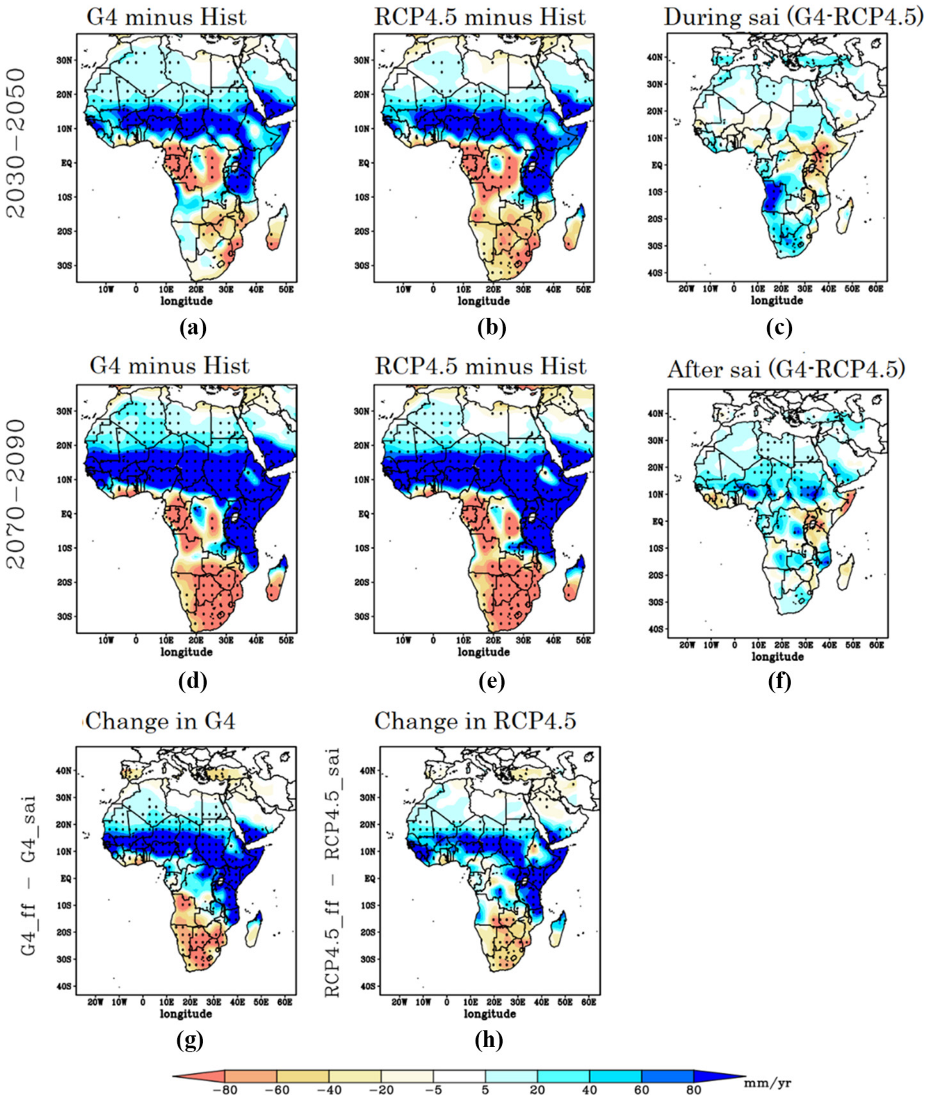

Figure A1.
Projected change in precipitation relative to historical period (1976–2005): for RCP4.5 (a) and (c) and for G4 (b) and (d)

Author affiliations

Salomon Obahoundje, African Centre of Excellence on Climate Change, Biodiversity and Sustainable Agriculture/LASMES, University Félix Houphouët Boigny, Abidjan, Cote D'ivoire

Vami Hermann N'guessan Bi, CURAT (University Center of Applied Research in Remote Sensing)/University Félix Houphouët-Boigny, Abidjan, Cote D'ivoire

Arona Diedhiou, African Centre of Excellence on Climate Change, Biodiversity and Sustainable Agriculture/LASMES, University Félix Houphouët Boigny, Abidjan, Cote D'ivoire, and Department of, Université Grenoble Alpes, IRD, Centre national de la recherche scientifique (CNRS), Grenoble Institut polytechnique de Grenoble (INP), Institut des Géosciences de l'Environnement (IGE), Grenoble, France

Ben Kravitz, Department of Earth and Atmospheric Sciences, Indiana University, Bloomington, Indiana, USA, and

John C. Moore, College of Global Change and Earth Systems Science, Beijing Normal University, Beijing, China and Arctic Center, University of Lapland, Rovaniemi, Finland

About the authors

Dr Salomon Obahoundje holds a PhD on Energy, Climate and Environmental Sciences at Felix Houphouët-Boigny University in Abidjan, Ivory Coast. His research works focus in climate-land-energy-water nexus in West Africa. He holds a BSc and an MSc in Physical Sciences, and a Master of Research on Climate Change and Energy from the West African Science Service Centre on Climate Change and Adapted Land Use (WASCAL) programme. His expertise is related to climate change impacts analysis, renewable energy, geoinformatics (GIS), remote sensing, watershed management, hydrologic and water resources modelling and simulation, as well as climate change and hydropower modelling. He is part of the WASCAL Alumna team involved in climate change and development at the local level. He has also contributed to the DFID/NERC "Future Climate for Africa" programme under AMMA-2050 project.

Dr Vami Hermann N'Guessan Bi is a Researcher at the University Center for Applied Research in Remote Sensing (Centre Universitaire de Recherche et d'Application en Télédétection (CURAT)) at Felix Houphouet-Boigny University in Abidjan, Ivory Coast. He has a PhD in Remote Sensing and GIS with a speciality in hydrogeology and climate. He is involved in several activities and projects in Africa. From February to September 2016, he worked as an Environment Quality Expert for a national agricultural project (PSAC-2016) funded by the World Bank, which aimed to introduce rural populations to best environmental practices. Since March 2017, he is a member of the national Technical Modelling Team for climate studies for the Low Emission Development Strategy-Africa project, funded by the European Union. Since April 2018; he is a Member of the GIS team for CLIMSUCAF project on the development of climate services for sugarcane farmers in Ivory Coast. Since December 2017, he is a Member of the GEMS-Africa (modelling of urban flooding hazard in a context of climate change) project's modelling team. Dr Vami Hermann N'Guessan Bi is the Principal Investigator of the GeoMIP-AFRICA supported by DECIMALS funds of the Solar Radiation Management Governance Initiative.

Dr Arona Diedhiou is a Research Director at "Institut de Recherche pour le Développement" (IRD) based at the "Institut des Géosciences de l'Environnement" (IGE, University of Grenoble-Alpes, France). He is hosted as a Visiting Scientist at the University Felix Houphouët Boigny (Abidjan, Côte d'Ivoire) as Co-director of the International Joint Laboratory NEXUS on interrelations between climate, water, agriculture and energy. He contributed to the coordination and the implementation of several international projects in Africa. Since 2021, he is Principal Investigator (PI) of SUSTAINDAM project (on the sustainable management and planning of hydropower in a context of climate and land use changes) implemented in the frame of the Belmont Forum collaborative actions on transdisciplinary research for pathways to

sustainability. Arona Diedhiou was Lead Author of the IPCC Special Report on the incidences of 1.5°C global warming and was Review Editor of the IPCC Assessment Report (WG1/AR6; Chapter 8 on changes in water cycle). Arona Diedhiou is the corresponding author and can be contacted at: arona.diedhiou@ird.fr

Dr Ben Kravitz is a Scientist Researcher on Control Systems Engineering and Climatology at the Department of Earth and Atmospheric Sciences, Indiana University, Bloomington, IN, USA, and Atmospheric Sciences and Global Change Division, Pacific Northwest National Laboratory, Richland, Washington, USA. His scientific research works are focused on solar geoengineering and climate change.

Dr John C. Moore is the Chief Scientist of College of Global Change and Earth System Science, Beijing Normal University and a Research Professor of Climate Change at Arctic Centre, University of Lapland, Finland. He is also a Member of Finnish Academy of Science and Letters, an Affiliate of Chinese Academy Sciences Center for Excellence in Tibetan Plateau Earth Sciences and a Guest Professor at the Polar Research Institute of China.